Molecular Crystals and Liquid Crystals
Publication details, including instructions for authors and subscription information:
http://www.tandfonline.com/loi/gmcl16

Freeze-Fracture Imaging of Ordered Phases of Tobacco Mosaic Virus in Water

Joseph A. N. Zasadzinski [a], Michael J. Sammon [a], Robert B. Meyer [b], M. Cahoon [c] & D. L. D. Caspar [c]
[a] AT&T Bell Laboratories, Murray Hill, New Jersey, 07974
[b] Martin Fisher School of Physics, Brandeis University, Waltham, Massachusetts, 02254
[c] The Rosenstiel Basic Medical Sciences Research Center, Brandeis University, Waltharn, Massachusetts, 02254
Version of record first published: 17 Oct 2011.

To cite this article: Joseph A. N. Zasadzinski , Michael J. Sammon , Robert B. Meyer , M. Cahoon & D. L. D. Caspar (1986): Freeze-Fracture Imaging of Ordered Phases of Tobacco Mosaic Virus in Water, Molecular Crystals and Liquid Crystals, 138:1, 211-229

To link to this article: http://dx.doi.org/10.1080/00268948608071761

Mol. Cryst. Liq. Cryst., 1986, Vol. 138, pp. 211–229
0026-8941/86/1384–0211/$20.00/0

Printed in the United States of America

Freeze-Fracture Imaging of Ordered Phases of Tobacco Mosaic Virus in Water

JOSEPH A. N. ZASADZINSKI and MICHAEL J. SAMMON

AT&T Bell Laboratories, Murray Hill, New Jersey 07974

ROBERT B. MEYER

Martin Fisher School of Physics, Brandeis University, Waltham, Massachusetts 02254

and

M. CAHOON and D. L. D. CASPAR

The Rosenstiel Basic Medical Sciences Research Center, Brandeis University, Waltham, Massachusetts 02254

(*Received February 8, 1986*)

Aqueous solutions of Tobacco Mosaic Virus are ideal systems for visualizing "molecular" distributions in nematic and crystalline phases by freeze-fracture electron microscopy. Nematic phases of TMV in water are highly oriented with measured order parameters of 0.93. Twist deformations appear to be most common in the micrographs, confirming experimental and theoretical evidence that the twist elastic constant is smaller than either the splay or bend constants. Both edge and screw disclinations are observed in TMV nematics at molecular resolution, and their overall configurations correspond closely to those predicted by continuum theory. Disclination cores have been visualized for the first time. The edge disclination core is small, no more than a single virus length wide. The virus reorient abruptly by 90° at the core, but appear to remain in the plane of the disclination line. The screw disclination core is several virus lengths in diameter and much more disordered. The virus twist out of the plane perpendicular to the line and into the plane along the disclination line. The virus in colloidal crystal TMV solutions are more positionally ordered than the nematic samples. Although no distinct layers were visible along the virus axis in the freeze-fracture images, a sinusoidal density modulation was observed. With the experimental evidence at hand, it is possible to assign either a smectic-B liquid crystal or a true three-dimensional crystal structure to this phase. Perpendicular to the long axis of the virus, the particles appear hexagonally ordered. An average center-to-center distance of 50 nm, which agrees with that measured by X-ray diffraction, was measured from the micrographs. Freeze-fracture imaging of these anisotropic crystals is an alternative to the more common light microscopy of polymer latex colloid crystals.

I. INTRODUCTION

Experimental[1–3] and theoretical[4] descriptions of how Tobacco Mosaic Virus (TMV) are distributed in water or dilute buffer solutions have been available for decades. Both colloidal crystal and nematic liquid crystal phases are formed by TMV in water, depending on the virus concentration, ionic strength, and pH.[5,6] The virus particles, each a rigid rod 320 nm long and 20 nm in diameter, are the structural equivalents of molecules in the more typical solid or thermotropic liquid crystals. The two orders of magnitude size increase between TMV and molecular solid and liquid crystals allows the "molecular" order in TMV solutions to be seen and interpreted using freeze-fracture replication transmission electron microscopy.

In freeze-fracture, a small volume of sample liquid is rapidly frozen, then fractured under vacuum to expose the interior structure. The fracture surfaces are replicated by evaporating platinum at an angle to highlight surface features, followed by carbon deposited normal to the fracture surface for mechanical strength. The platinum-carbon replicas are then examined in a transmission electron microscope. Point-to-point resolution in an ideal replica is limited by the size of the platinum grains in the shadowing film and is approximately 2 nm.

Freeze-fracture has been used extensively in biological studies of membrane structure and cellular organization.[7] However, freeze-fracture of colloidal dispersions has advanced less quickly because the necessary freezing rates were unavailable.[8] Unless freezing is rapid enough to cause vitrification of the surrounding ice matrix, growing ice crystals displace colloidal particles to the crystal grain boundaries and disrupt the dispersion. New rapid freezing techniques[9] apparently are able to vitrify the surrounding water matrix,[10] thus preventing any displacement of the colloidal particles. Therefore, it is now possible to visualize the distribution and orientation of individual virus particles in ordered aqueous phases without freezing artifacts or chemical treatments.

II. EXPERIMENTAL

Monodisperse samples of Tobacco Mosaic Virus (TMV) were prepared by the method of Boedtker and Simmons.[3] Tobacco plants were infected with common strain (Vulgare) TMV when the plants were eight weeks old. The leaves were harvested after two to three weeks, then frozen, pulverized and the sap removed by straining.

After straining, the virus were separated from the plant sap by differential centrifugation. The pH and ionic strength of the sap were controlled using phosphate buffers.

Virus dispersed in deionized water exhibited Bragg diffraction of visible light, evidence of regular layers,[5,6] while virus dispersed in buffer appeared birefringent between crossed polars, indicating nematic order.[6] A thin (< 50 microns) film of sample liquid was prepared by trapping a small drop (0.1–0.5 μl) between two copper planchettes (Balzers, Hudson, New Hampshire) in a humidity controlled glovebox. The samples were allowed to equilibrate between the copper sheets for three to five minutes. Preliminary experiments showed that plunging the specimen sandwich into liquid freon (Figure 1a) or liquid propane (Figure 1b) allowed ice crystals to grow and forced the virus to collect at grain boundaries. However, samples frozen between the opposed high velocity streams of liquid propane

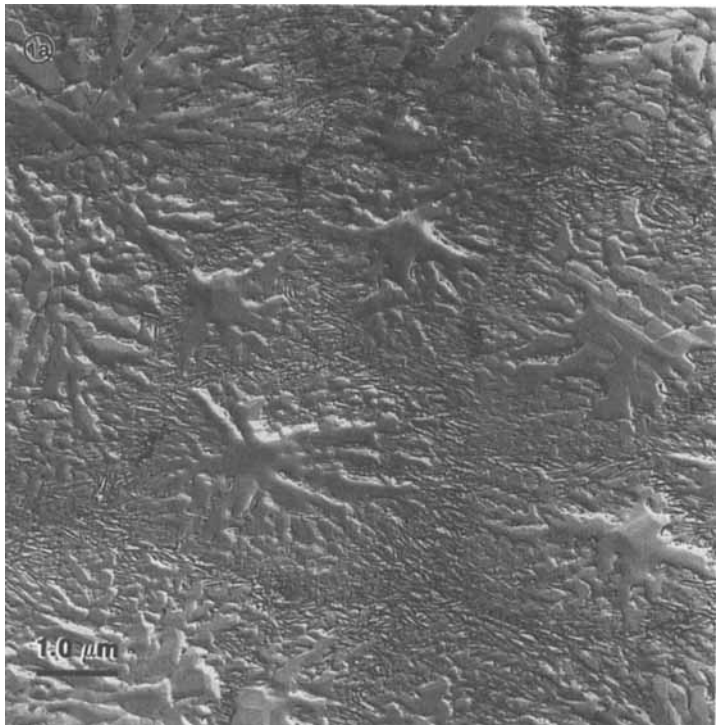

FIGURE 1a 10 wt% TMV in water-nematic solution frozen by plunging into liquid-solid freon slush cooled by liquid nitrogen. Large, radial ice crystals have displaced the TMV to the grain boundaries.

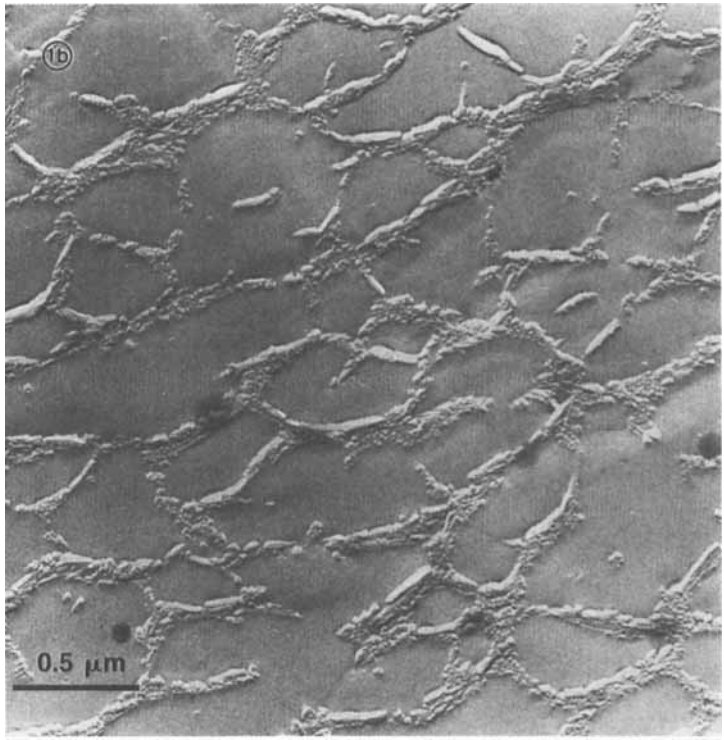

FIGURE 1b Same as (a) except frozen by plunging into liquid propane cooled by liquid nitrogen. Ice crystals are smaller, but TMV are still displaced to the grain boundaries.

in a Balzer's cryo-jet apparatus[9] showed no signs of ice crystal formation or virus aggregation (Figure 1c). As a check of the freezing process, a TMV nematic sample containing 20% ethylene glycol (which inhibits ice crystallization)[7] was prepared and imaged (Figure 1d). Other than a rougher background fracture surface in the sample containing ethylene glycol, there were no differences in the distribution or locations of the virus particles.

Jet-frozen specimens were fractured at $-170°C$ and 10^{-8} torr, then replicated with platinum/carbon in a Balzers 400 freeze-etch unit. Typically, 1.5 nm of platinum, controlled by an oscillating quartz crystal monitor, was deposited at a 45° angle, followed by 10 nm of carbon deposited normal to the fracture surface. The samples and replicas were removed from the bell jar and brought to room temperature. To free the replicas, the copper planchettes were slowly dissolved in chromic acid,[11] leaving the replicas suspended at the

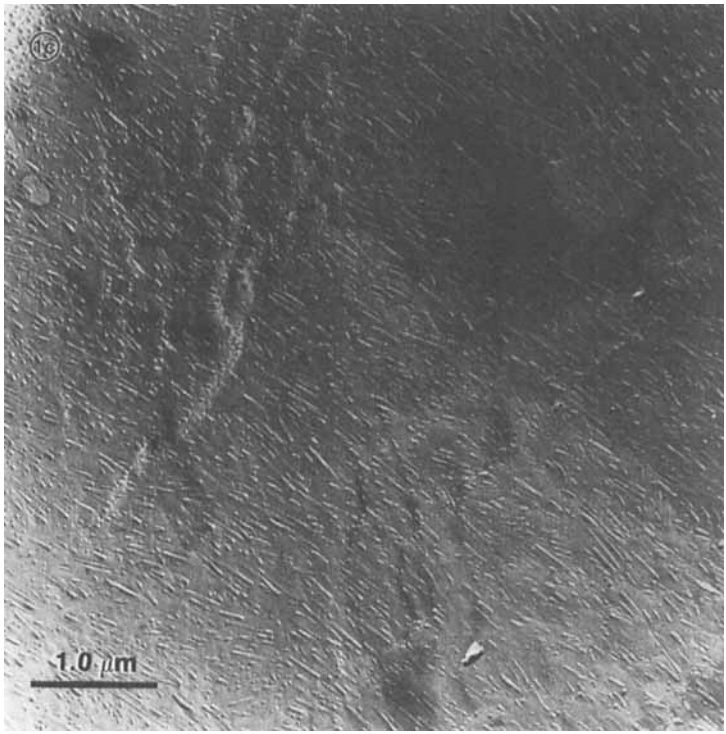

FIGURE 1c Same as (a) except jet-frozen by high velocity opposed streams of liquid propane. No evidence of ice crystallization or displacement of virus.

liquid interface. The replicas were washed in deionized, doubly distilled water, collected on forvmar-coated 50 mesh gold grids (Ted Pella, Tustin, California), and examined in a JEOL 100B STEM in the conventional transmission mode. Shadows (absence of platinum) appear light in the prints. In some of the micrographs, residue from the virus or impurities in the cleaning fluids show up as irregular dark patches. These patches detract only from the cosmetic value of the micrographs and do not alter the virus distribution or orientation in the replica.

III. OBSERVATIONS

TMV nematics

Images of freeze-fracture replicas of TMV nematics show that the virus are well ordered over many virus lengths (Figure 2). Many of

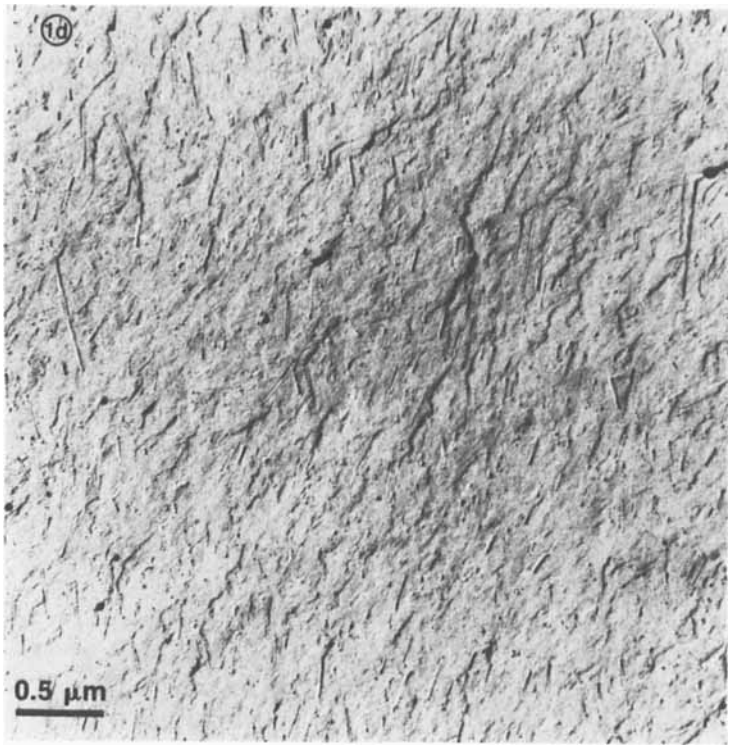

FIGURE 1d TMV nematic containing 20% ethylene glycol as cryoprotectant to inhibit crystallization. Although the background fracture surface is much rougher than in (c), the distribution and orientations of the virus appear similar.

the virus cross-fracture through their centers, and show the 4 nm diameter central hole down the axis of the virus. The fine striations normal to the virus axis visible in many of the micrographs are the helical arrays of individual protein sub-units that make up the outer shell of the virus.[6] Resolution in the replicas is about 2 nm, the limit imposed by the platinum grains. Many of the virus appear to lie entirely in the fracture plane in Figure 2; the average length of these in-plane virus is 320 nm, and the standard deviation is 17 nm, confirming that the virus population is monodisperse.

An estimate of the order parameter, S, of the TMV nematic was obtained by measuring the projected length of the in-plane virus along the average orientation (N in the micrograph), then dividing by the total length of the virus. This determines $\cos\theta$, in which θ is the angle of deviation of an individual virus from the average direction. The

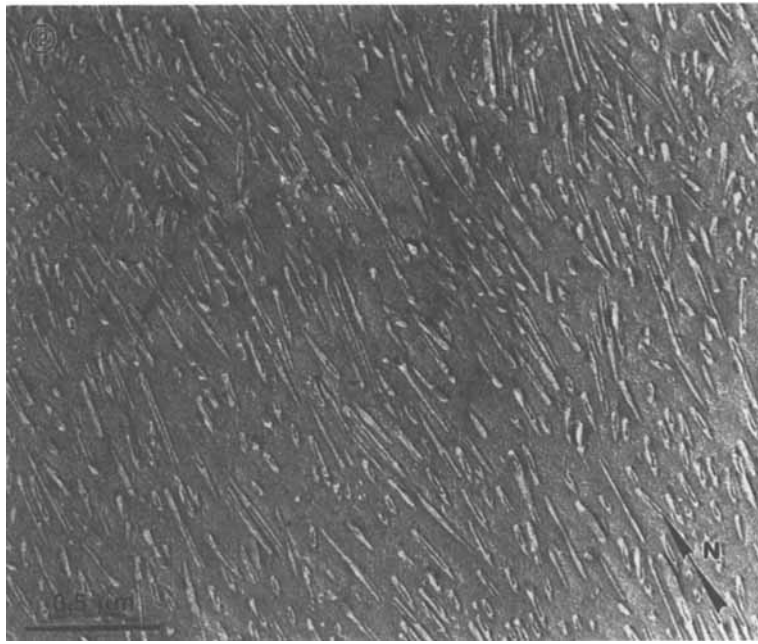

FIGURE 2 Well-ordered region of TMV nematic. Average length of virus is 320 ± 17 nm. N is the director. The order parameter is 0.93.

order parameter is defined in the usual way:[12]

$$S \equiv 1/2\langle(3\cos^2\theta - 1)\rangle$$

For the in-plane virus in Figure 2, S is 0.93, which agrees well with the 0.9 measured by preliminary X-ray studies.[13] As expected, the order parameter measured over small areas is greater than the bulk value measured by X-ray. However, because any artifacts of freezing tend to decrease the order, the agreement between the two methods suggests that the freezing rate is high enough to prevent the virus from rearranging.

The virus align parallel to the bounding surfaces of the copper planchettes used to form the specimens as seen in Figure 3; however, no preferred orientation in the plane of the copper surface seems to be imposed. Each virus appears to be oriented mainly by its closest neighbors; small bundles of virus are nearly parallel to each other, but misoriented with respect to the other bundles. One reason for

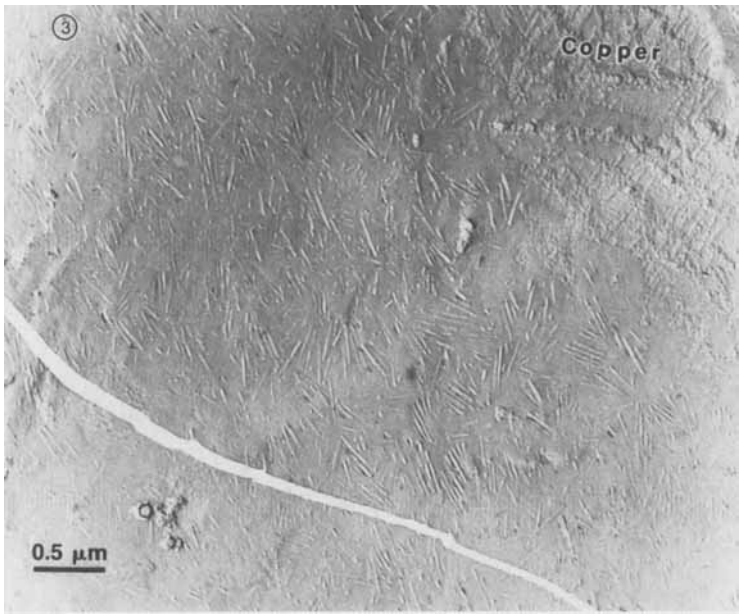

FIGURE 3 TMV nematic fractured near the copper planchette. Virus appear to align parallel to the copper surface, but have no preferred orientation in the plane. Virus in "bundles" (circled) are parallel, but misoriented with respect to adjacent bundles.

this is that the copper surface is rough and irregular with many micron-sized projections. The virus bundles often fit into one of the pits in the copper surface and are cut off from the rest of the virus in the bulk. It is likely that the virus in the bulk of the sample are aligned by flow when the sample is prepared.

Figure 4 shows the TMV nematic perpendicular to the long axis of the virus. The individual particles appear as light, unshadowed circular rings with a dark interior spot. If the dark spot is centered on a uniform, circular ring, the virus is perpendicular to the fracture surface. The virus particles do appear to line up in rows in certain areas of the micrograph, but overall, the center-to-center spacing is not uniform. It is unusual for the TMV nematic to present this large of a perpendicular fracture surface because the fracture usually propagates parallel to the copper planchettes and the virus align parallel to these surfaces. (See Figure 3.)

Distortions in the direction of local molecular orientation in TMV nematics require little energy, as in thermotropic nematics. All distortions in a nematic phase are the sum of three principal modes:

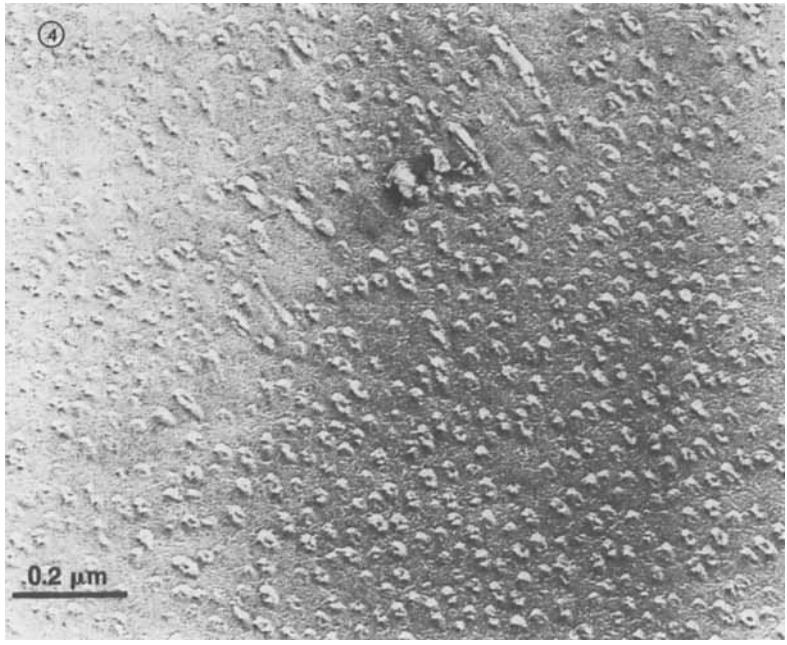

FIGURE 4 End-on view of TMV nematic. The virus appear to line up in irregular rows, but do not appear equally separated.

splay, twist, and bend (Figure 5a), each with its associated elastic constant.[14,15] Theoretical values of the elastic constants can be computed from the rigid-rod theory of Onsager.[4,16] For highly oriented nematics such as TMV, Onsager theory predicts that the bend elastic constant is large in comparison to the splay and twist constants. Experimentally, K_2, the twist constant, is of the order 10^{-7} dynes/cm, K_1, the splay constant, is about 5 times as large, and K_3, the bend constant, is about 40 times K_2.[17]

Figure 5b shows regions in the TMV nematic in which each of the three principle modes of deformation is visible. Twist deformations are most common and are manifested as a rotation of the virus out of the fracture plane. Twist deformations seem to occur more often and over a shorter distance than either splay or bend deformations which suggests that the twist elastic constant is smallest. In splay and bend deformations, the virus remain in the plane of the director.

Disclinations in TMV nematics

Disclinations are line defects around which the molecular orientation changes discontinuously and are well described by singular solutions

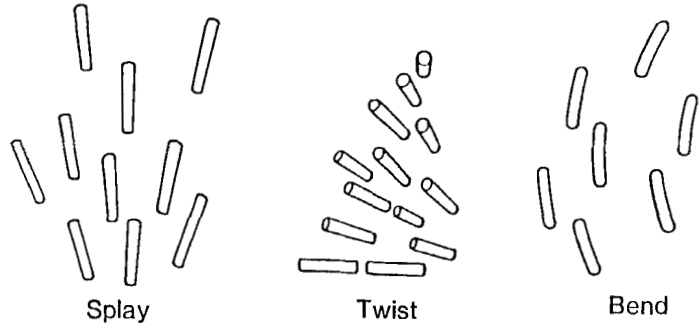

FIGURE 5a Three principal modes of deformation in liquid crystals.

of the continuum equations of Oseen[14] and Frank.[15] Two types of disclinations exist; edge (or twist) disclinations, which have their rotation axis perpendicular to the disclination line, and screw (or wedge) disclinations, which have their rotation axis parallel to the disclination line. (See Figures 6, 7a, b.)[12] However, the continuum equations

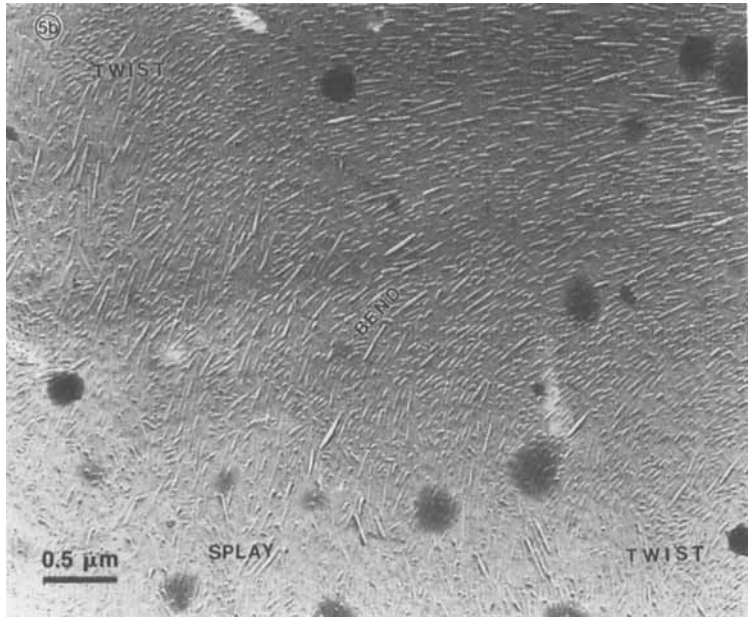

FIGURE 5b TMV nematic showing regions that can be classified as one of the three principal modes. Note that twist, which involves rotating the virus out of the fracture plane, appears most common, and occurs over the shortest distances.

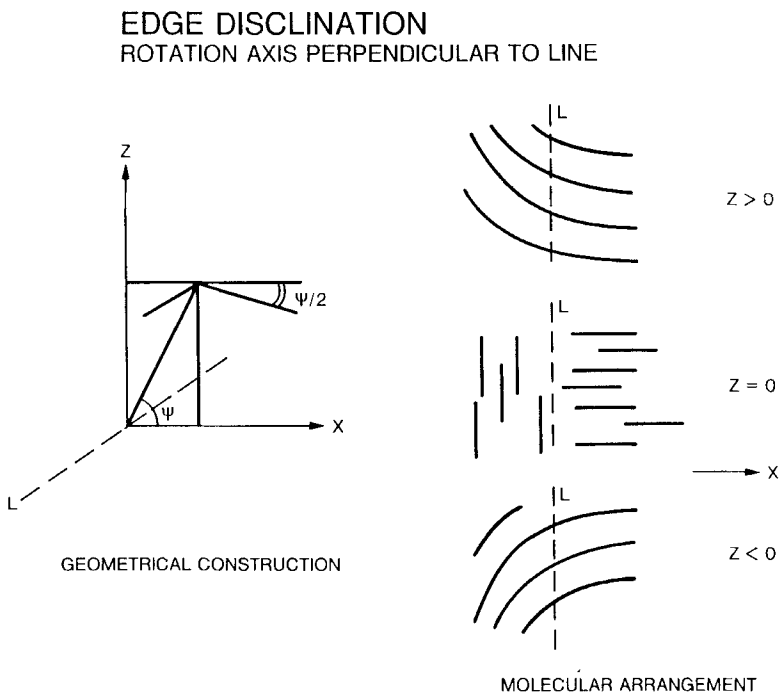

FIGURE 6 Geometrical construction and molecular arrangement of a |1/2| edge disclination (after deGennes).[12]

cannot describe the molecular configuration near the core of the defect.

Figure 8 shows a TMV nematic sample fractured near a |1/2| edge disclination line. The virus particles abruptly change orientation by 90° along the disclination line, similar to the drawing in Figure 6. The disclination core is narrow, never appearing to be more than one virus in width. There appear to be small pockets of water (arrowed) along the core, possibly to fill in any gaps in the virus arrangements, thereby relieving any regions of large stress. The thermotropic nematic analog to the patches of water may be local variations in density at the disclination core; however, the virus distribution is not isotropic near the core.

Figure 9 shows a $-1/2$ screw disclination line almost perpendicular to the fracture plane. The molecular configuration around the line is similar to Figure 7b. However, near the core of the disclination, the virus appear much more disordered and seem to twist out of the fracture plane (arrows). The core of the screw disclination is several

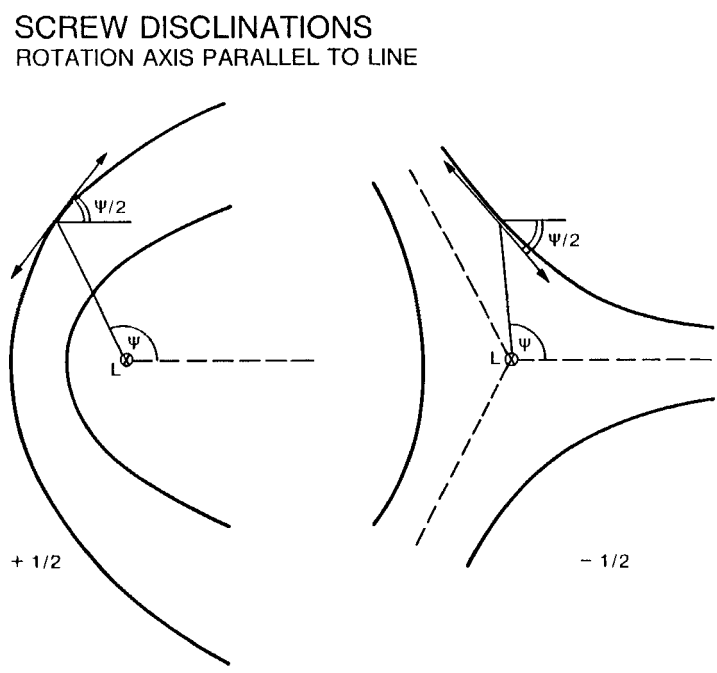

FIGURE 7a, 7b Geometrical construction of screw disclinations. The local molecular axis follows the heavy black lines. The disclination and rotation axis are perpendicular to the page.

virus wide. As the energy of a disclination increases with the size of the core,[18] Figures 8 and 9 suggest that edge disclinations are of lower energy than screw disclinations, and hence would be more numerous. The deformation around a screw disclination line involves splay and bend, which are higher energy processes, as compared to the deformation around an edge disclination line, which involves mainly twist. The rigid virus particles cannot bend at sufficiently sharp angles as required near the core of the $-1/2$ screw disclination; therefore, the core of the defect is large and the virus must twist out of plane to provide the necessary curvature. On the other hand, twist does not require any distortion of the virus, even for large deformations, hence the core of the edge disclination is small. In bulk samples of TMV observed in a light microscope, edge disclination loops are the predominant defects.[6]

Colloidal crystals

Figure 10 is an image of a replica of a sample of TMV colloidal crystal. About every 5–10 microns, the fracture surface abruptly

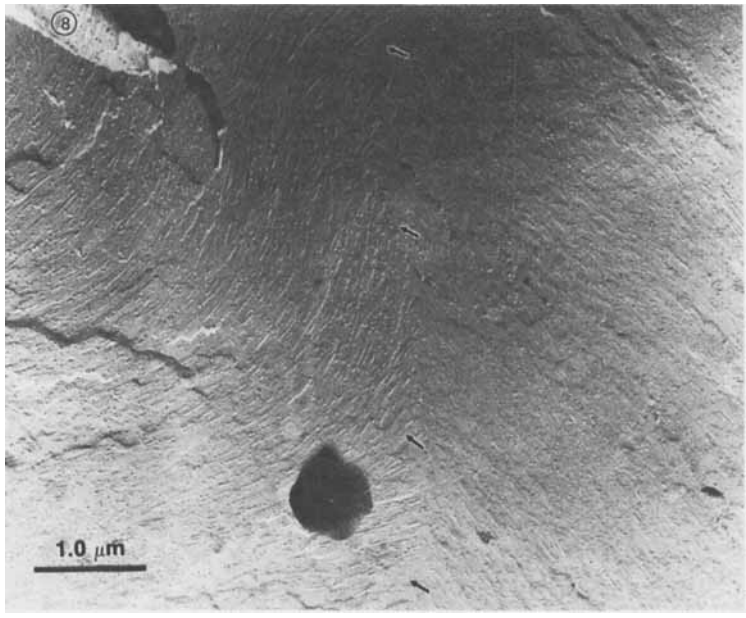

FIGURE 8 Twist disclination in a TMV nematic. The virus abruptly rotate by 90° along the disclination line which is in the center of the micrograph from top to bottom. Small pockets of water (arrows) seem to fill in gaps along the core, which appears to be no more than one virus wide.

changes direction; on one side, the virus are nearly parallel to the fracture surface and on the other, nearly perpendicular. These abrupt changes may be evidence of grain boundaries between misoriented crystallites of the virus. Kreibig and Wetter estimated the crystallite size to be from 3 to 12 microns by analyzing the diffraction peak width observed by light scattering.[5] The virus appear to be better ordered over longer distances than in the nematic phase, and the side-to-side spacing is more uniform.

An enlarged view of the arrowed area of Figure 10 (Figure 11) shows that the centers of mass along the rows of virus extending from left to right across the micrograph appear to be correlated. The layering is not perfect due to three factors. First, thermal fluctuations displace the virus along the direction of its axis. The forces that lead to the formation of layers are smaller and less directed than those responsible for the orientational order and side-to-side spacing. Layers may not exist in reality; there may exist only a sinusoidal density modulation as in smectic liquid crystals. One way of testing this is by diffracting light from the TMV layers. Smectic-like order results in

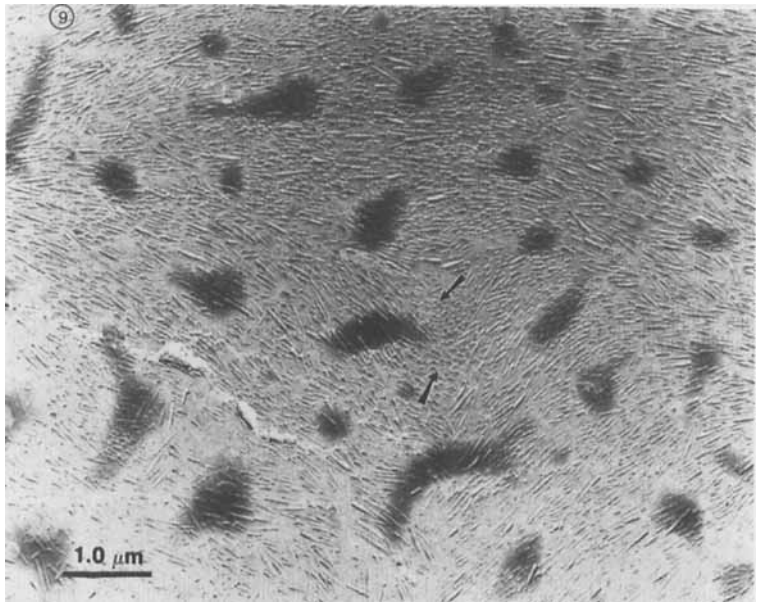

FIGURE 9 −1/2 Screw disclination in a TMV nematic. The core of the screw disclination appears larger than in the edge disclination and is also more disordered. The virus appear to twist out of the fracture plane along the disclination line (arrows).

only a single Bragg reflection, while crystal layers give higher order reflections. Only first order reflections have been observed in TMV colloidal crystals.[3,5] It is not known whether higher order reflections do exist because the wavelengths required to obtain these reflections are inaccessible or cause the virus to absorb strongly. It is therefore possible that TMV colloid crystals are more like smectic B liquid crystals, which have hexagonal order in the plane but only a sinusoidal density modulation perpendicular to the plane,[19] than true crystals.

The second factor that contributes to the apparent imperfections in the layering is the fracture process. There is no control over the propagation of the fracture front, and no reason to expect that any particular virus orientation is a preferred fracture direction. The fracture surfaces are rough and irregular as can be seen by the varying shadows across Figures 10 and 11. Small changes in the direction of fracture could result in significant deviations in the apparent layering or in the apparent lattice arrangement when the virus are viewed end-on. The fracture surface bounces from one plane of virus to another and presents various oblique as well as parallel fractures

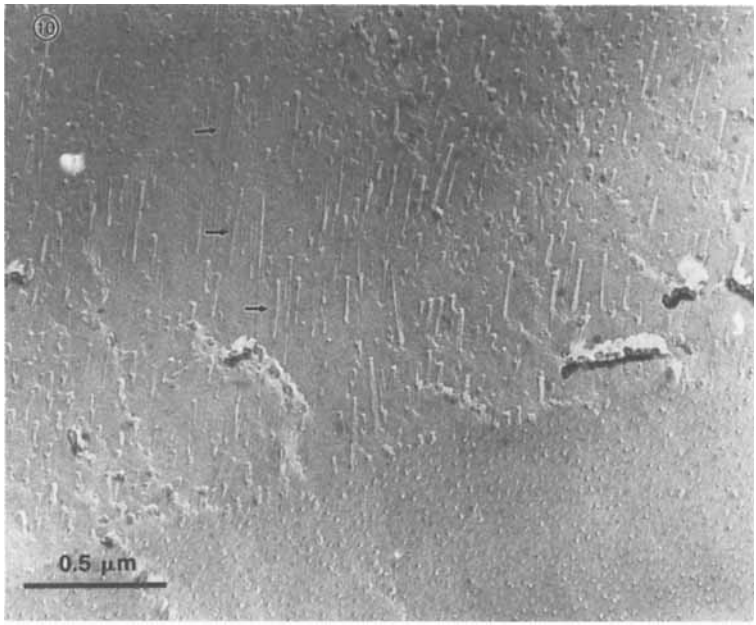

FIGURE 10 Replica of TMV colloidal crystal sample near an apparent grain boundary at which the virus change directions.

through the virus. Allowing the ice matrix to sublimate or "etch" might reveal a more regular arrangement underlying the fracture surface. Such experiments are planned for the near future. Figure 12 shows more uniform layers of TMV; however, the fracture plane is oblique to the virus axis and the ends of many of the virus have broken off, confusing the actual structure.

The third factor is that because colloid crystals are soft, the shear involved in making the sample sandwiches likely disrupts the order in the samples. In future experiments, the samples will be allowed to anneal for a longer time between the copper sheets before jet-freezing.

Viewed end-on in Figure 13, the virus are more uniformly spaced than in the nematic phase, with a center-to-center distance of about 50 nm, which agrees with the spacing measured by small-angle X-ray diffraction.[2] At least two orders of reflection have been observed from the hexagonal lattice with X-rays and the reflections appear sharp,[2] indicating that the hexagonal pattern is distinct and extends over distances that are large in comparison to the lattice spacing. In

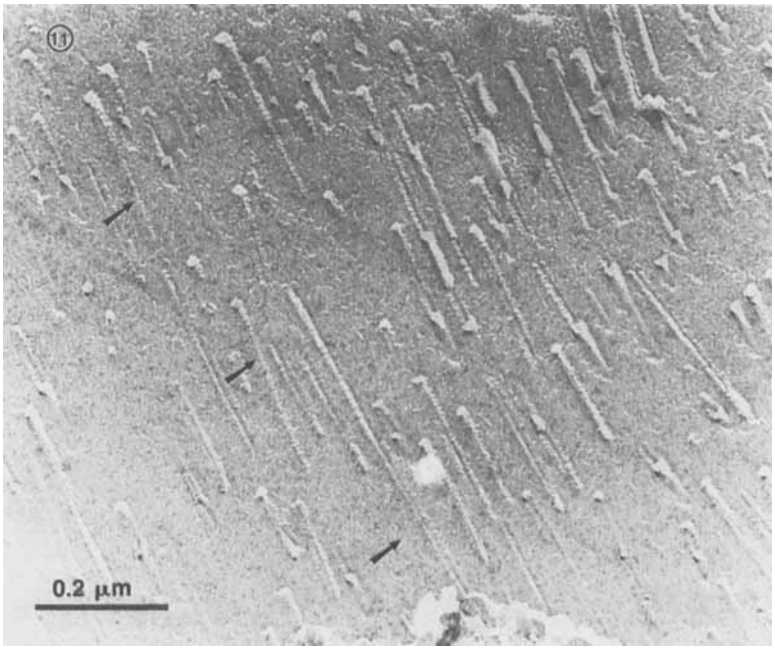

FIGURE 11 Enlarged view of the boxed area of Figure 10. Note the regular density modulation along the virus axis, but the absence of any real layers. Spacing between the arrows is about 340 nm.

the freeze-fracture micrographs, the virus appear to be well ordered over large distances, but the hexagonal pattern is not distinct. Usually, one can distinguish two sets of rows in the micrographs, at various angles to each other (along the arrows in Figure 13). Around many of the virus, six nearest neighbors can be found in nearly the correct positions. It appears that the hexagonal ordering of the virus perpendicular to their long axis is less affected by sample preparation than the ordering into rows along the virus axis.

IV. CONCLUSIONS AND FURTHER WORK

Aqueous solutions of Tobacco Mosaic Virus are ideal systems for visualization of molecular order in nematic and crystalline phases by freeze-fracture electron microscopy. Rapid freezing of thin (< 50 microns) samples is essential to prevent the growth of ice crystals and the resulting disruption of the distribution, orientation and structure of the virus particles. Replication of the fracture surface with platinum

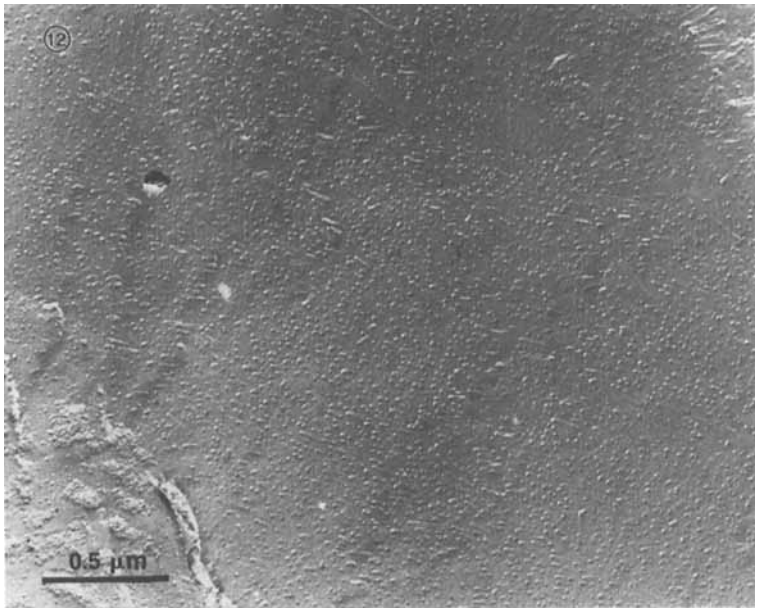

FIGURE 12 Low magnification view of colloidal crystal sample Fracture plane is oblique to the virus axis. The layers are poorly defined, but a density modulation along the virus axis is visible.

and carbon gives sufficient contrast to observe the patterns of the protein sub-units helically arranged along the virus axis, a resolution of about 2 nm. It should be possible to visualize almost any colloid dispersion of rigid particles with freeze-fracture to this resolution.

Nematic phases of TMV in water are highly oriented with measured order parameters of 0.93. Twist deformations appear to be most common in the micrographs, confirming experimental and theoretical evidence that the twist elastic constant is smaller than either the splay or bend constants. Both edge and screw disclinations are observed in TMV nematics at molecular resolution, and their overall configurations correspond closely to those predicted by continuum theory. With the molecular resolution possible in these model systems, disclination cores have been visualized for the first time. The edge disclination core is small, no more than a single virus length wide, and seems to be decorated with small patches of excess water. The virus reorient abruptly by 90° at the core, but appear to remain in the plane of the disclination line. The screw disclination core is several virus lengths in diameter and much more disordered. The virus twist out

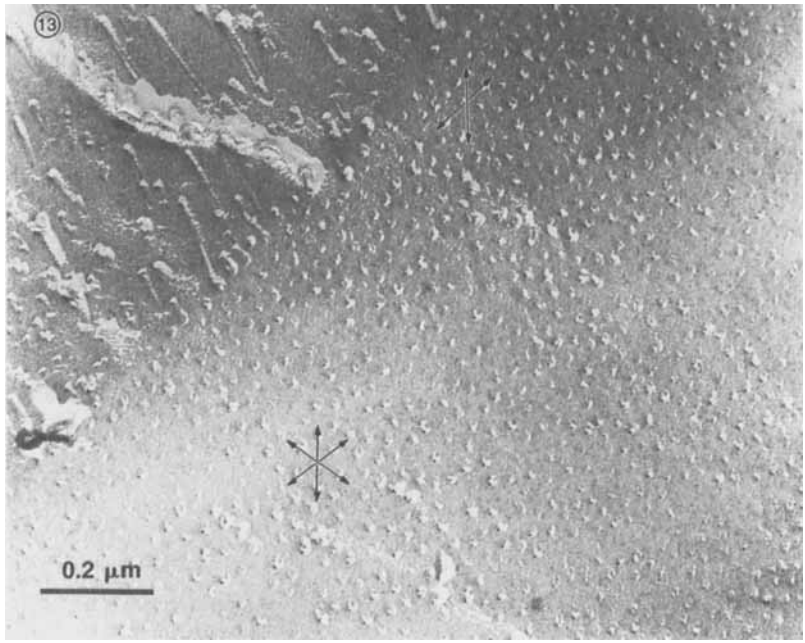

FIGURE 13 End-on view of colloidal crystal sample. Local hexagonal packing is present, but the lattice is distorted by the irregularities of the fracture. Two rows of well aligned virus are along the arrows. Center-to-center spacing is about 50 nm.

of the plane perpendicular to the line and into the plane along the disclination line. The relative sizes of the cores suggest that the edge disclinations have lower energy than screw disclinations. This is consistent with light microscopy observations that show edge disclinations to be the predominant defect.

The virus in colloidal crystal TMV solutions have better positional order than the nematic samples. Although no real layers were visible along the virus axis in the freeze-fracture images, a sinusoidal density modulation was observed. With the experimental evidence at hand, it is possible to assign either a smectic-B liquid crystal or a true three-dimensional crystal structure to this phase. Perpendicular to the long axis of the virus, the particles appear hexagonally ordered, but the fracture plane always appears to cut the lattice obliquely and the imaged arrangement appears distorted. An average center-to-center distance of 50 nm, which agrees with X-ray measurements, is obtained from the micrographs.

Additional experiments are planned to improve the freeze-fracture results. The perturbing influence of the fracture process may be elim-

inated by etching several hundred Angstroms of ice from the fracture surface prior to replication to reveal the structure underlying the fracture plane. The influence of shear during the creation of the copper sandwich samples might be removed by allowing the samples to anneal for longer times. By digitizing and analyzing the micrographs, we hope to obtain quantitative information including order parameters, autocorrelation functions, and radial distribution functions for the nematic and crystalline TMV solutions.

Acknowledgments

I am grateful for helpful discussions with S. Meiboom, D. W. Berreman, and P. E. Cladis. The technical expertise and patience of Dr. M. J. Costello of Duke University were also deeply appreciated.

References

1. S. C. Bawden and N. W. Pirie, *Proc. Royal Soc. London, B.* **123**, 274 (1937).
2. J. D. Bernal and I. Fankuchen, *J. Gen. Physiology*, **25**, 111 (1941).
3. H. Boedtker and N. S. Simmons, *J. Am. Chem. Soc.*, **80**, 2550 (1958).
4. L. Onsager, *Ann. N. Y. Acad. Sci.*, **51**, 627 (1949).
5. U. Kreibig and C. Wetter, *Z. Naturforsch.*, **35c**, 750 (1980).
6. S. Fraden, A. J. Hurd, R. B. Meyer, M. Cahoon, and D. L. D. Caspar, *J. Physique (Paris) Coll.*, **46**, C3-85 (1985).
7. J. E. Rash and C. S. Hudson, *Freeze Fracture: Methods, Artifacts, and Interpretations*, (Raven Press, New York, 1979), pp. 37–195.
8. R. Menold, B. Luttge and U. Kaiser, *Adv. Colloid and Interface Sci.*, **5**, 281 (1976).
9. M. Muller, N. Meister and H. Moor, *Mikroscopie (Wien)*, **36**, 129 (1980).
10. M. Adrian, J. Dubochet, J. Lepault and A. W. McDowall, *Nature* **308**, 32 (1984).
11. M. J. Costello, R. Fetter and M. Hochli, *J. Microscopy (Oxford)*, **125**, 125 (1983).
12. P. G. deGennes, *The Physics of Liquid Crystals*, (Oxford University Press, Oxford, 1974) pp. 23–34, 125–131.
13. R. Oldenbourg, R. B. Meyer, M. Cahoon and D. L. D. Caspar, unpublished data.
14. C. W. Oseen, *Trans Faraday Soc.*, **29**, 883 (1933).
15. F. C. Frank, *Disc. Faraday Soc.*, **25**, 19 (1958).
16. J. P. Straley, *Phys. Rev.*, **A8**, 2181 (1973).
17. A. J. Hurd, S. Fraden, F. Longerg and R. B. Meyer, *J. Physique (Paris)* **46**, 905 (1985).
18. S. Meiboom, J. P. Sethna, P. W. Anderson and W. F. Brinkman, *Phys. Rev. Let.*, **46**, 1216 (1981).
19. S. Chandrasekhar, *Liquid Crystals*, (Cambridge University Press, Cambridge, 1977) pp. 274–285.